

PHYSICAL REVIEW D

PARTICLES AND FIELDS

THIRD SERIES, VOL. 2, NO. 1

1 JULY 1970

K^\pm -Proton Elastic Cross Sections at 180° from 0.41 to 0.72 GeV/c*

P. K. CALDWELL, T. BOWEN, F. NED DIKMEN, E. W. JENKINS, R. M. KALBACH, D. V. PETERSEN, AND A. E. PIPER

Department of Physics, University of Arizona, Tucson, Arizona 85721

(Received 11 March 1970)

The K^\pm - p elastic scattering was measured in a small angular region near 180° ($-0.995 \leq \cos\theta^* \leq -1.0$) at six momenta from 0.41 to 0.72 GeV/c. The forward-scattered protons were detected with scintillation counters and identified by time-of-flight measurements. The K^+ - p elastic differential cross section at 180° is found to be essentially constant with a value near 0.9 mb/sr. The sum of the P -wave phase shifts ($2\delta_{3/2} + \delta_{1/2}$) is found to be negative in this momentum region. The K^- elastic differential cross section is found to dip to a minimum (0 ± 0.2 mb/sr) at 0.66 GeV/c.

I. INTRODUCTION

THIS experiment has measured the backward elastic K^\pm - p scattering in the momentum range 0.41–0.72 GeV/c. We have used counter techniques to measure the differential cross section in the angular region $-1.0 \leq \cos\theta^* \leq -0.995$ as a function of the laboratory momentum of the kaon, where θ^* is the c.m. scattering angle. Sufficient data were taken in increments of 0.06 GeV/c to achieve statistical errors of about 10% in K^+ scattering, and 25% or 0.2 mb/sr in K^- - p scattering.

The π^\pm - p and K^\pm - p scattering in the extreme backward direction has previously been studied above 1.0 GeV/c.^{1,2} Below 1.0 GeV/c, however, information about the backward scattering must be inferred from complete angular distributions measured with bubble chambers or spark chambers.³ Such experiments often

do not measure in the backward direction beyond 160° , or combine all of the data between 160° and 180° as a single point.

Section II contains a description of the experimental apparatus. The corrections necessary to extract the cross sections from the raw data are briefly discussed in Sec. III. In Sec. IV the K^+ results are used to test the usual hypothesis that low-energy K^\pm - p scattering is isotropic.

II. METHOD AND APPARATUS

In the momentum range 0.41–0.72 GeV/c the recoil kaon from an elastic scattering near 180° has a range in liquid hydrogen of less than 10 cm. At 0.40 GeV/c, the range is less than 2 cm. Therefore, since a target length of about 45 cm was chosen to obtain a reasonable counting rate, the elastic differential cross section at 180° was measured by detecting the forward-going protons. These were separated electronically from residual beam particles, principally by time-of-flight measurements. Additional separation was provided by a threshold Čerenkov counter and by energy-loss (dE/dx) measurements.

Counters

The counters and beam arrangement are shown schematically in Fig. 1. The beam incorporated one stage of electrostatic separation with a first focus at counter S_1 and a second focus at counter S_4 . S_1 and C_0 were located within the mass- and momentum-selecting jaws at the first focus. S_2 , C_1 , S_3 , and G were beam-defining counters placed in front of the hydrogen target. All incoming beam particles were identified by signals

* Work supported in part by a grant from the National Science Foundation.

¹ A. S. Carrol, J. Fischer, A. Lundby, R. H. Phillips, C. L. Wang, F. Lobkowicz, A. C. Melissinos, Y. Nagashima, C. A. Smith, and S. Tewksbury, Phys. Rev. Letters **23**, 887 (1969).

² S. W. Kormanyos, A. D. Krisch, J. R. O'Fallon, K. Ruddick, and L. G. Ratner, Phys. Rev. Letters **16**, 709 (1966); A. S. Carroll, J. Fischer, A. Lundby, R. H. Phillips, C. L. Wang, F. Lobkowicz, A. C. Melissinos, Y. Nagashima, and S. Tewksbury, *ibid.* **20**, 607 (1968).

³ A few examples are W. R. Holley, E. F. Beall, D. Keefe, L. T. Kerth, J. J. Thresher, C. L. Wang, and W. A. Wenzel, Phys. Rev. **154**, 1273 (1967); L. A. Bertanza, A. Bigi, R. Carrara, R. Casali, R. Pazzi, D. Berley, E. L. Hart, D. C. Rahm, W. J. Willis, S. S. Yamamoto, and N. S. Wong, *ibid.* **177**, 2036 (1969); M. B. Watson, M. Ferro-Luzzi, and R. D. Tripp, *ibid.* **131**, 2248 (1963); S. Goldhaber, W. Chinowsky, G. Goldhaber, W. Lee, T. O'Halloran, T. F. Stubbs, G. M. Pjerrou, D. H. Stork, and H. K. Ticho, Phys. Rev. Letters **9**, 135 (1962).

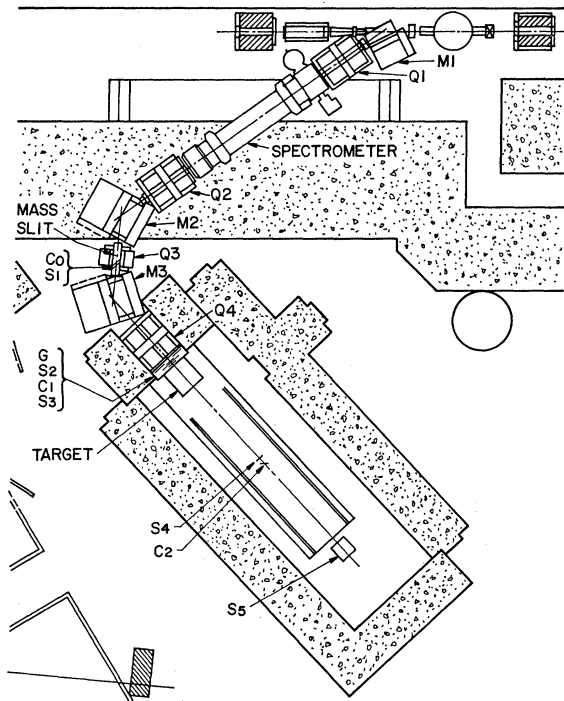


FIG. 1. Layout of the partially separated K^\pm beam, including the bending magnets ($M1-M3$), the quadrupoles ($Q1-Q4$), and the placement of the counters. The experimental area was enclosed in concrete shielding to reduce background.

from scintillation counters S_1 , S_2 , and S_3 . Protons in the K^+ beam were rejected by dE/dx measurements in S_1 and S_2 , by electrostatic separation, and by time of flight. S_1 and S_2 were separated by a distance of 10 ft. Pions, muons, and electrons in the beam were rejected by Čerenkov counters C_0 and C_1 , by time of flight, and by electrostatic separation. The guard counter G vetoed off-axis particles.

Protons produced in the forward direction were detected by scintillation counter S_4 . This counter was

5 in. diam and defined the solid angle within which events were accepted. S_4 was placed in fast coincidence with the remainder of the proton telescope, C_2 and S_5 , in order to reject kaon beam particles. S_5 was 17 ft from the target and provided time-of-flight information to enhance the separation of event particles. The scintillator of this counter was 2 in. thick with a photomultiplier tube placed directly behind to provide isochronous light collection. This arrangement reduced timing variations due to the geometry of S_5 to ± 0.25 nsec. S_4 and S_5 were also used to reject beam particles by providing dE/dx measurements, since the kaon pulse height was typically ≤ 0.75 of the pulse height corresponding to an event. C_2 was a Lucite Čerenkov counter mounted at 60° to the beam line (75° was used at the highest momentum). This counter rejected any remaining pion, muon, or electron contamination, and rejected some kaons at momenta above $0.5 \text{ GeV}/c$. Light from the faster particles was reflected internally into the photomultiplier tube, while any light generated by the event protons was lost through the downstream face of the counter.

Target

The target assembly consisted of two identical cylindrical Mylar flasks 18 in. long and 6 in. diam enclosed in an aluminum box. One flask was filled with liquid hydrogen and the other was used as a dummy target for background determinations. Provision was made for rapid positioning of either flask in the beam from a remote station. The target length was chosen so as to provide a sufficient counting rate, without stopping protons from 180° elastic scattering in the extreme upstream end of the target. It was also desired to keep the momentum loss of the kaons in the target at a minimum. Kaons which enter the target of $0.43 \text{ GeV}/c$ exit at about $0.39 \text{ GeV}/c$. This spread diminishes as the momentum increases and is less than $20 \text{ MeV}/c$ at an incident momentum of $0.72 \text{ GeV}/c$. The effective

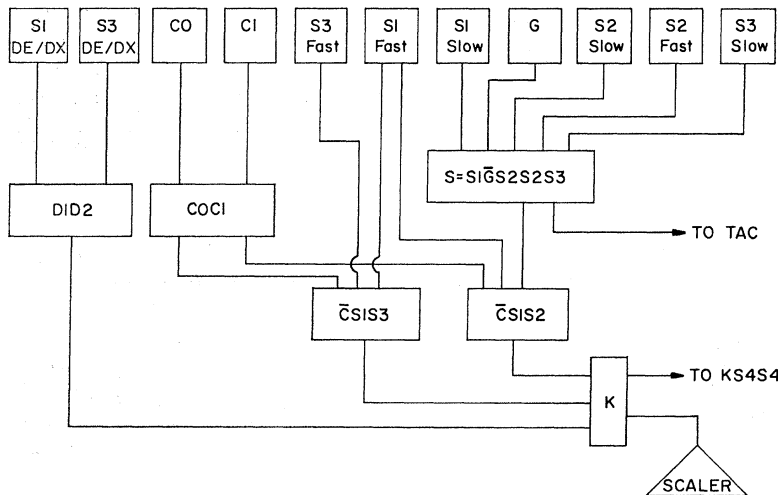


FIG. 2. Block diagram of the logic which identified the incident kaons.

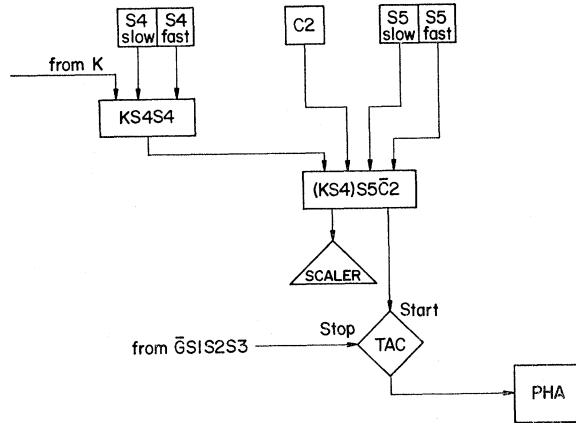


FIG. 3. Block diagram of the logic which identified and analyzed probable events.

length of the target was determined by a consideration of the physical dimensions of the flask and the measured beam distribution, and was found to be 44.6 cm.

Electronics: Kaon Identification

Logic circuitry for the beam telescope is shown schematically in Fig. 2. Signals from scintillation counters S_1 , S_2 , and S_3 were each split and fed into two discriminators labeled "fast" and "slow" corresponding, respectively, to low- and high-level discrimination. This technique provided good leading-edge timing from the "fast" discriminators and noise rejection from the "slow" discriminators.

Slow signals from S_1 , S_2 , and S_3 together with S_2 fast and G were fed into a 200-MHz coincidence circuit which is labeled S . This coincidence signal was initiated by S_2 fast and preserved the S_2 time information. The S_3 slow discriminator was of the updating variety and the output signal of 50 nsec was clipped to 10 nsec. The net result is that the electronics is insensitive to any second beam particle which follows within 60 nsec of the first.

The coincidence circuits $S_1S_3\bar{C}$ and $S_1S_2\bar{C}$ identified kaons by time of flight and included fast-particle rejection by means of Lucite Čerenkov counters C_0 and C_1 . The final kaon coincidences $K\bar{D}$ included the two preceding coincidences and provided rejection of beam protons or two simultaneous particles (doubles) by S_1 and S_3 dE/dx .

This arrangement of counters and electronics reduced the beam contamination due to pions, muons, and electrons to less than 0.3% in the K^- beam, and to less than 0.05% in the K^+ beam. Proton contamination in the K^+ beam is reduced to 0.2% at 0.72 GeV/c, and decreases with momentum. The principal rejection against beam protons is time of flight, with the dE/dx rejection providing an extra factor of 3 to 5 depending upon the momentum.

Electronics: Forward Proton Identification

Figure 3 shows the electronics used to detect the forward-going protons. The dE/dx and time-of-flight information from S_4 are analyzed by KS_4S_4 . $(KS_4)S_5\bar{C}_2$ includes the dE/dx information from S_5 slow and the fast-particle rejection of C_2 , and the output pulse is initiated by S_5 fast. The proton telescope rejected the noninteracting beam particles by a factor of 10^5 at the lower momenta, with a factor of 10 due to dE/dx measurements and the remainder due to the time-of-flight rejection of S_4 . At higher momenta these mechanisms became less effective, but C_2 became operational so that, at 0.72 GeV/c, a rejection factor of 10^4 against beam kaons was still possible.

When an event passed all of the logic requirements, S_5 fast started the time-to-amplitude converter (TAC). The TAC was then stopped by the output of S_2 fast, which had been appropriately delayed. The TAC information was then stored in a pulse-height analyzer (PHA). The total resolution of the system was such that the peaks due to beam kaons or protons generated by turning off the appropriate rejection logic had full widths at half-maximum amplitude of less than 2 nsec (8 channels). The PHA was used to analyze all particles which passed the logic requirements. The PHA contents along with the scaler reading of the number of incoming kaons constituted the raw data. An example of the PHA contents is shown in Fig. 4.

III. DATA REDUCTION AND ANALYSIS

The following contaminations of the raw data were considered: (1) beam kaons not rejected by the proton telescope, (2) beam protons misidentified as incident K^+ , (3) inelastic events in the case of K^- such as $K^- + p \rightarrow \Sigma + \pi$, (4) background due to possible second particles accompanying a beam kaon, and (5) π^\pm - p elastic scatterings at 180° . In most cases the true events

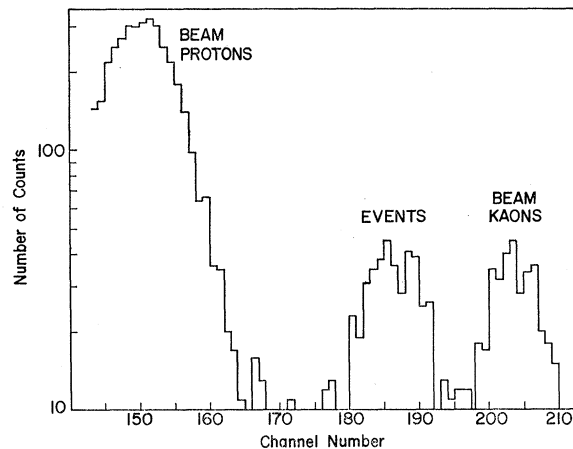


FIG. 4. Time-of-flight spectrum for K^+ at a laboratory momentum of 600 MeV/c. The K^- data were similar, but lacked the large peak due to proton contamination in the beam.

TABLE I. K^+ - p data.

P_{lab} (GeV/c)	N_{events}	F	$E\Delta\Omega$	$\sigma_{\text{tot}}/4\pi$ Ref. 4	$d\sigma/d\Omega$ (180°) (mb/sr)
0.407	113±14	0.876	0.00734	1.080±0.025	0.92±0.13
0.477	234±23	0.890	0.00767	1.070±0.014	0.91±0.11
0.539	260±21	0.902	0.00791	0.985±0.016	0.90±0.08
0.600	315±26	0.910	0.00809	1.030±0.015	1.14±0.11
0.660	186±30	0.918	0.00835	0.973±0.016	0.85±0.15
0.721	194±42	0.923	0.00856	0.888±0.020	0.87±0.19

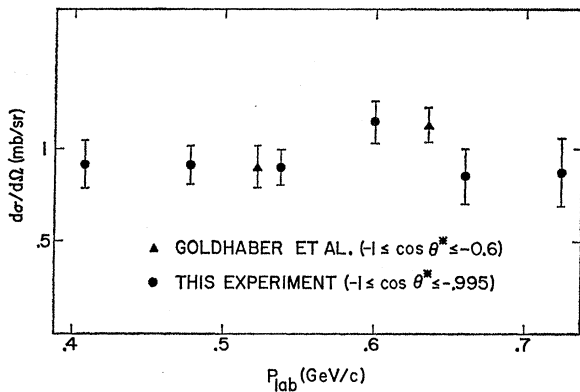
TABLE II. K^- - p data.

P_{lab} (GeV/c)	N_{events}	F	$E\Delta\Omega$	$d\sigma/d\Omega$ (180°) (mb/sr)
0.407	56±11	0.83	0.00734	4.05±0.84
0.477	64±13	0.86	0.00765	1.72±0.36
0.539	30±7	0.88	0.00791	0.77±0.18
0.600	11±10	0.89	0.00810	0.2 ±0.2
0.660	-4±10	0.90	0.00835	0.0 ±0.2
0.721	35±17	0.90	0.00856	0.55±0.28

give a well-resolved peak in the S_2 - S_5 time-of-flight spectrum, although the K^+ data at 0.72 GeV/c did require unfolding by a computer program to distinguish the events from the K^+ and beam proton peaks on either side. The fitting was done by assuming all peaks to be Gaussian with known centers, and adjusting the areas and widths to obtain an optimum fit.

The peaks due to beam kaons and misidentified beam protons could always be positively identified by turning off an appropriate rejection mechanism and allowing sufficient data to accumulate in the PHA. These peaks were also seen in the empty-target data, while peaks corresponding to events were seen only in the full-target area. Events due to π^\pm - p scatters were not distinguishable from K^\pm - p scatters. However, such contamination of the beam was always less than 0.3%, as discussed previously. Peaks due to inelastic events are not evident in any K^+ data. Any extraneous peaks which might be expected in the K^- data and which might be identified as inelastic events would not be as well constrained kinematically as the elastic peak and would represent a broad background in the PHA spectrum. Some background was observed but the peak corresponding to events was always clearly distinguishable.

The number of events counted at each momentum is the number of events in the peak minus a background derived from the empty-target data. In the case where a fit was made by computer, the empty-target background was fitted and the parameters obtained were

FIG. 5. K^+ results shown with the bubble-chamber data of Goldhaber *et al.*

then used in fitting the full-target data. The number of events with statistical errors becomes

$$N_{\text{full}} - \zeta N_{\text{empty}} \pm (N_{\text{full}} + \zeta^2 N_{\text{empty}})^{1/2},$$

where N_{full} is the number of events observed in the full target running, N_{empty} is the background to be subtracted, and ζ is the ratio of incident beam on full target to incident beam on empty target.

The differential cross section at 180° is calculated from the following equation:

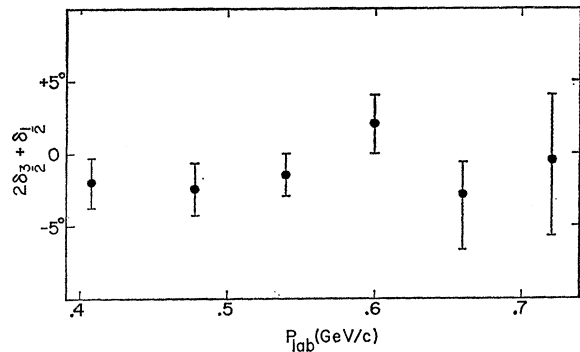
$$d\sigma/d\Omega = k \times N(\text{events}) / [N(\text{kaons}) \times F \times E\Delta\Omega],$$

where k , a geometrical factor, is 535 mb, and $E\Delta\Omega$ is the efficiency-solid-angle product of the system and is defined as

$$E\Delta\Omega = 2\pi \int_0^\pi E(\theta^*) \sin\theta^* d\theta^*,$$

where $E(\theta^*)$ is the efficiency as a function of scattering angle. The factor F given in the equation above is a correction for the loss of beam kaons either by decay or by nuclear scattering in the target region. The factors F and $E\Delta\Omega$ are given in Tables I and II.

The factor $E\Delta\Omega$ was computed by a Monte Carlo technique and included the effects of multiple Coulomb and nuclear scattering of the protons in the target and in counters S_4 and C_2 . It was found that only events for which $\cos\theta^* \leq -0.995$ were observable. We were able to experimentally confirm the Monte Carlo calculation by using beam protons to simulate event protons.

FIG. 6. Calculated values of $2\delta_{3/2} + \delta_{1/2}$, using the present 180° data and the total cross sections of Bowen *et al.*

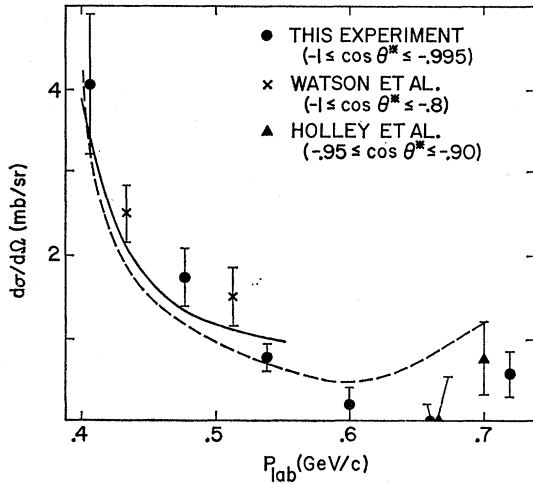


FIG. 7. K^- results shown with the bubble-chamber data of Watson *et al.* and spark-chamber data of Holley *et al.* The errors shown on the data of Watson *et al.* are based on the number of events in the backward bin only. The dashed and solid lines are explained in the text.

IV. RESULTS AND DISCUSSION

The K^+p elastic differential cross sections are given in Table I and shown in Fig. 5. The statistical errors are on the order of 10–15%. Systematic errors are estimated to be less than 2%. The cross section is essentially structureless. If the scattering were pure S wave, then the total and differential cross sections would be related by

$$d\sigma/d\Omega = \sigma_{\text{tot}}/4\pi. \quad (1)$$

K^+p scattering is known to be almost purely elastic below 0.65 GeV/ c . Our data indicate that even as low as 0.4 GeV/ c , as indicated in Table I, where no inelastic

processes are possible, the S -wave approximation is not completely valid. The fact that our differential cross sections lie slightly below the prediction for pure S -wave scattering indicates that the P -wave amplitudes interfere destructively with the S wave. The S wave is known to be repulsive and the P -wave amplitude must also be repulsive in order to agree with the experiment. Using the results of this experiment together with the recent total cross-section measurements of Bowen *et al.*,⁴ the total P -wave phase shift ($2\delta_{3/2} + \delta_{1/2}$) was calculated. The necessary assumptions are that only S and P waves are present, and that the amount of P wave is small. The results of this calculation are shown in Fig. 6.

The K^-p elastic differential cross sections are given in Table II and shown in Fig. 7. The statistical errors are on the order of 25% or ± 0.25 mb. The K^-p cross section shows a pronounced dip at 0.66 GeV/ c . The solid line in Fig. 7 is from the multichannel effective-range fit of Kim⁵ to the previous data in the region 0–550 MeV/ c . The dashed line is our own fit using Kim's parameters with the addition of the amplitudes of higher-mass direct channel resonances. The parameters of the resonances were taken from Refs. 1 and 6.

ACKNOWLEDGMENTS

We wish to acknowledge the members of the Bevatron staff and crew, in particular, W. Hartsough, for their cooperation. We also wish to thank T. Elioff for his advice and encouragement during the experiment.

⁴ T. Bowen, P. K. Caldwell, F. N. Dikmen, E. W. Jenkins, R. M. Kalbach, D. V. Petersen, and A. E. Pifer (unpublished).

⁵ J. K. Kim, Phys. Rev. Letters 19, 1074 (1967).

⁶ N. Barash-Schmidt, A. Barbaro-Galtieri, L. R. Price, A. H. Rosenfeld, P. Söding, C. G. Wohl, M. Roos, and G. Conforto, Rev. Mod. Phys. 41, 109 (1969).